

# Allylic C–H Difluoroalkylation of Unactivated Alkenes with Trifluoromethylarenes

Tiancen Bian, Nils W. Melbourne, Yi Liu, Guilhem Colomer, Rui Sun, Marcus A. Tius, and Zuxiao Zhang\*



Cite This: *ACS Catal.* 2025, 15, 13039–13047



Read Online

ACCESS |



Metrics & More



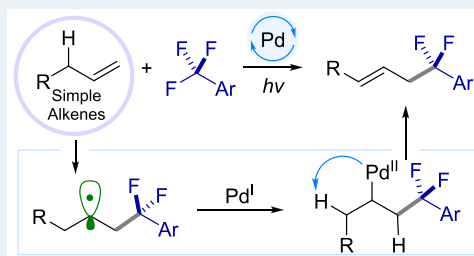
Article Recommendations



Supporting Information

**ABSTRACT:** We disclose a redox-neutral, visible-light-induced palladium-catalyzed allylic C–H difluoroalkylation of unactivated alkenes using trifluoromethylarenes as readily available electrophilic fluoroalkylating agents. The transformation proceeds via photoinduced C–F bond cleavage to generate difluorobenzyl radicals, which undergo an allylic Mizoroki–Heck-type cascade with regioselective  $\beta$ -hydride elimination. The *gem*-difluoromethylene unit plays a crucial role in directing regiochemistry, potentially by stabilizing key Pd(II) intermediates. This protocol operates under mild conditions, exhibits a broad substrate scope, and enables late-stage functionalization, providing a practical platform for the modular incorporation of bioactive difluoroalkyl groups into olefinic frameworks.

**KEYWORDS:** allylic C–H difluoroalkylation, hybrid palladium catalysis, unactivated alkenes, selective defluorination, late-stage functionalization



## INTRODUCTION

Allylic C–H functionalization of simple alkenes stands as a straightforward and step-efficient method for synthesizing functionalized alkenes. Over the past two decades, significant advancements have been made in this field, offering powerful tools for direct C–H to C–C and C–X bond conversions.<sup>1–4</sup> Meanwhile, the incorporation of difluoromethylene (–CF<sub>2</sub>–) units into organic molecules has attracted substantial attention in pharmaceutical and agrochemical research, due to their ability to modulate key physicochemical properties such as lipophilicity, hydrogen bonding, and metabolic stability.<sup>5</sup> Given these features, direct allylic C–H difluoroalkylation of unactivated alkenes represents a highly attractive yet underexplored approach to access partially fluorinated, structurally diverse molecules from simple olefinic precursors. Despite this appeal, several challenges have hindered the development of such a transformation. Classical strategies for allylic C–H functionalization generally proceed via two mechanistic paradigms. In one approach, palladium-catalyzed C–H activation generates electrophilic allyl–Pd(II) intermediates, which undergo substitution with various soft nucleophiles in the presence of an external oxidant.<sup>2</sup> Alternatively, nucleophilic allylmetal species – derived from late transition metals (Fe, Co) or alkali metals (Li, Na) – can add to polarized  $\pi$ -electrophiles under basic conditions.<sup>3</sup> However, these approaches<sup>4</sup> are generally incompatible with difluoroalkylation, due to the absence of suitably reactive difluoroalkylating reagents that can engage in effective cross-coupling with  $\pi$ -allyl or anionic intermediates (Figure 1a).

To circumvent this limitation, recent studies have employed radical-mediated strategies (Figure 1b). For example, electrophilic reagents such as Togni-type compounds or hypervalent iodine/CF<sub>2</sub>HCO<sub>2</sub>H combinations have been used to access allylated products via radical or carbocationic intermediates.<sup>6</sup> While enabling, these protocols rely on highly reactive reagents, limiting their generality and scalability. More recently, Lei and co-workers reported a cobalt/photoredox-catalyzed difluoroalkylation of alkenes, enabling allylic functionalization of terpenes through halogen- and hydrogen-atom transfer with 2-bromo-2,2-difluoroacetate.<sup>7</sup> In parallel, Fu and co-workers developed a cobalt-catalyzed, ligand-controlled regiodivergent Heck-type reaction of unactivated alkenes and fluoroalkyl bromides, affording either vinyl or contra-thermodynamic allylic products depending on the reaction conditions.<sup>8</sup> While these advances significantly expand the toolbox for fluoroalkylation, these approaches remain constrained by the limited availability and tunability of fluoroalkylating reagents (e.g., CF<sub>3</sub>, CF<sub>2</sub>H, CF<sub>2</sub>CO<sub>2</sub>R), restricting broader application to diverse difluoroalkyl units.

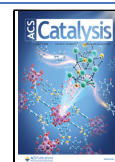
Inspired by the emerging field of hybrid palladium catalysis,<sup>9,10</sup> particularly Zhang's seminal contributions to

Received: June 10, 2025

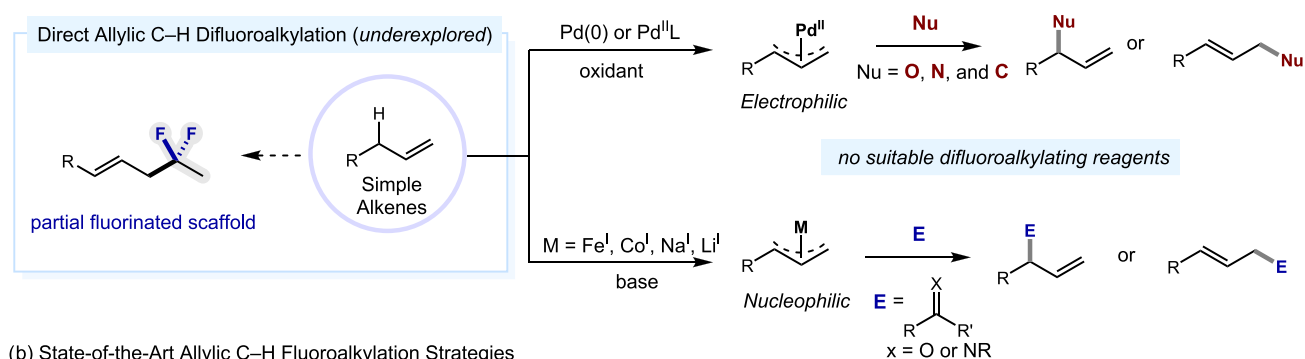
Revised: July 8, 2025

Accepted: July 9, 2025

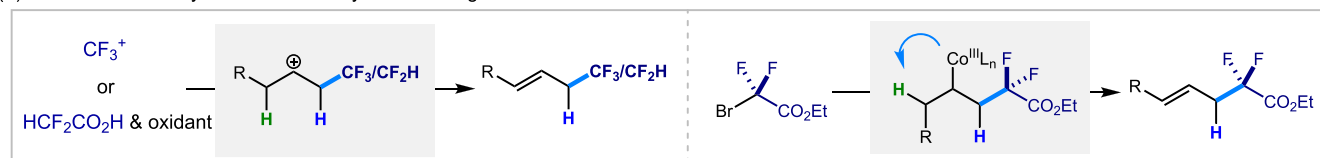
Published: July 16, 2025



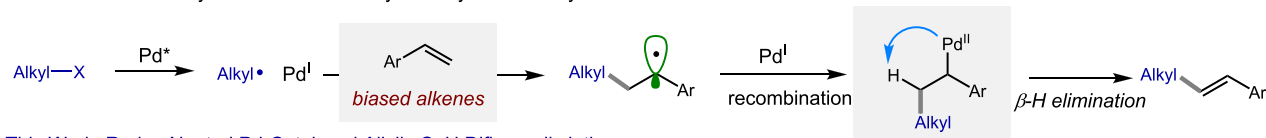
## (a) Allylic C–H functionalization of simple alkenes



## (b) State-of-the-Art Allylic C–H Fluoroalkylation Strategies



## (c) Recent advances of Hybrid Palladium Catalyzed alkylation of vinylarenes via formal Mizoroki–Heck Reactions



## (d) This Work: Redox-Neutral Pd-Catalyzed Allylic C–H Difluoroalkylation

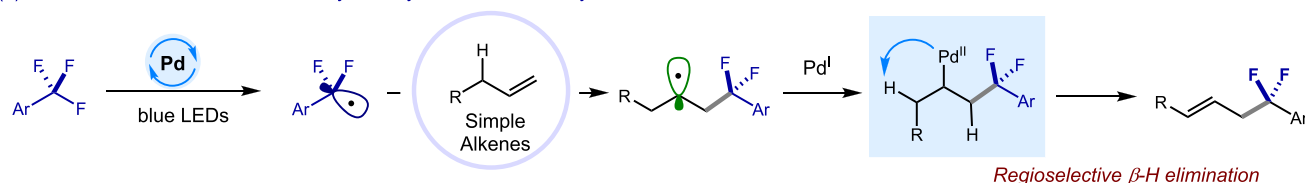


Figure 1. Background and reaction design.

visible-light-induced palladium-catalyzed C–F bond arylation of trifluoromethylarenes,<sup>11</sup> we and others have subsequently expanded this area by developing hybrid palladium-catalyzed difunctionalizations of conjugated dienes via C–F bond cleavage.<sup>12</sup> Building on these insights, we questioned whether redox-neutral allylic C–H difluoroalkylation could be achieved using readily available trifluoromethylarenes ( $\text{Ar-CF}_3$ ) as electrophilic coupling partners. Prior studies have shown that photoexcited  $\text{Pd(0)}$  can activate  $\text{Ar-CF}_3$  via single-electron transfer (SET) to generate difluorobenzyl radicals under visible light.<sup>11,12</sup> We envisioned that such radicals could be intercepted by unactivated alkenes in a formal Mizoroki–Heck-type cascade, enabling direct allylic C–H difluoroalkylation. Although hybrid Pd-catalyzed Mizoroki–Heck reactions have been demonstrated for vinylarenes (Figure 1c),<sup>10</sup> to our knowledge, no example has been reported for Pd-catalyzed alkyl allylic Heck-type functionalization of unactivated alkenes.<sup>13</sup> A key challenge lies in controlling regioselectivity during  $\beta$ -hydride elimination: alkyl– $\text{Pd(II)}$  intermediates derived from unactivated alkenes often contain multiple  $\beta$ -hydrogens of similar steric and electronic environments, leading to regioisomeric mixtures.<sup>14</sup> To address this challenge, we hypothesized that the installed gem-difluoromethylene moiety could serve as a directing element – through both steric and electronic effects, and possibly via  $\text{Pd-F}$  coordination – to enforce regioselective  $\beta$ -hydride elimination.<sup>15</sup> Herein, we report a redox-neutral, hybrid Pd-catalyzed allylic C–H difluoroalkylation of unactivated alkenes using trifluoromethylarenes as electrophilic fluoroalkylating agents.

This strategy enables the construction of valuable difluoroalkylated allylarenes with high regioselectivity under mild and operationally simple conditions (Figure 1d).

## METHODS

To test our hypothesis, we selected ethyl 4-methylenecyclohexane-1-carboxylate (**1a**) and (3,5-bis(trifluoromethyl)phenyl)methanol (**1b**) as model substrates for reaction optimization (Table 1). The ester and hydroxyl groups were strategically incorporated to enhance the product polarity, facilitating isolation. Initially, subjecting these substrates to the reaction conditions with  $\text{Pd(PPh}_3)_4$  as the catalyst,  $\text{Cs}_2\text{CO}_3$  as the base, and  $N,N$ -dimethylformamide (DMF) as the solvent under 10W blue LED irradiation yielded the desired product in 10%, with no detectable vinyl byproducts (entry 7). Optimizing the base (entries 1–7) identified potassium formate ( $\text{HCOOK}$ ) as a superior alternative, significantly increasing the yield to 75%. Solvent screening (entries 8–9) confirmed DMSO as optimal, whereas alternatives like dioxane led to diminished yields. Increasing the loading of  $\text{Pd(PPh}_3)_4$  did not improve yields, suggesting that catalyst concentration was not a limiting factor (entry 10–12). Further optimization involved increasing the light intensity to 40 W blue LEDs, which accelerated the reaction and improved the yield to 86% (entry 13). However, the reductive Mizoroki–Heck reaction became the dominant side pathway, likely due to the reducing nature of the formate. To mitigate this, various potassium bases were screened and potassium acetate ( $\text{AcOK}$ ) was found

Table 1. Optimization of Conditions<sup>a</sup>

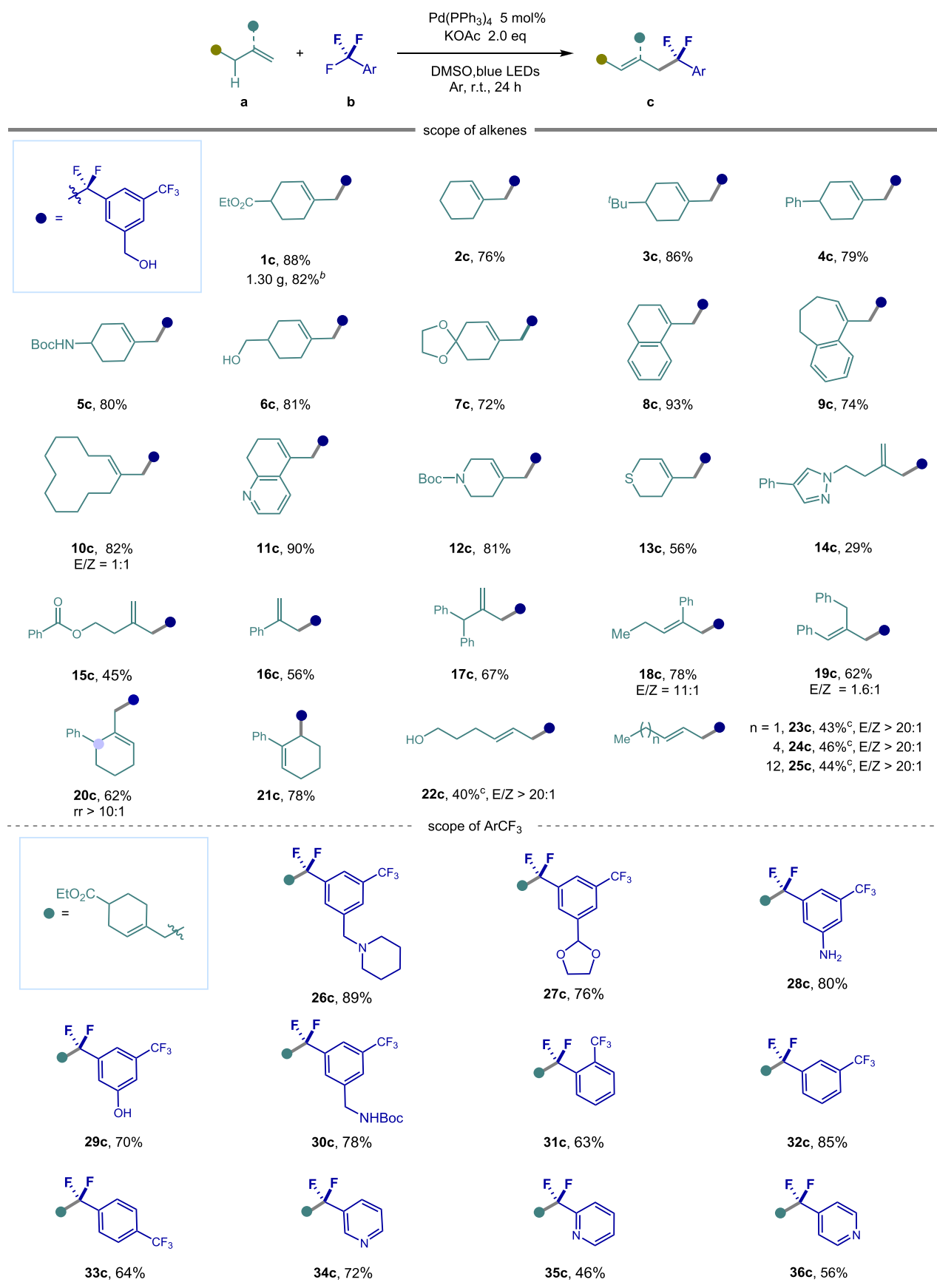
entry	Pd(PPh <sub>3</sub> ) <sub>4</sub>	base	solvent	<b>1c</b> yield [%]
1	5 mol %	HCOOK	DMF	75
2	5 mol %	K <sub>3</sub> PO <sub>4</sub>	DMF	32
3	5 mol %	K <sub>2</sub> HPO <sub>4</sub>	DMF	55
4	5 mol %	KH <sub>2</sub> PO <sub>4</sub>	DMF	32
5	5 mol %	Na <sub>2</sub> CO <sub>3</sub>	DMF	13
6	5 mol %	NaHCO <sub>3</sub>	DMF	10
7	5 mol %	Cs <sub>2</sub> CO <sub>3</sub>	DMF	10
8	5 mol %	HCOOK	DMSO	73
9	5 mol %	HCOOK	dioxane	3
10	7.5 mol %	HCOOK	DMF	71
11	10 mol %	HCOOK	DMF	71
12	12.5 mol %	HCOOK	DMF	72
13 <sup>b</sup>	5 mol %	HCOOK	DMF	80
14 <sup>b</sup>	5 mol %	AcOK	DMSO	86
15 <sup>c</sup>	5 mol %	AcOK	DMSO	95(88 <sup>d</sup> )
16	0 mol %	AcOK	DMSO	NR
17 <sup>e</sup>	5 mol %	AcOK	DMSO	NR

<sup>a</sup>General conditions (unless otherwise specified): **1a** (0.1 mmol), **1b** (0.2 mmol), Pd(PPh<sub>3</sub>)<sub>4</sub> (5 mol %), Base (0.2 mmol), solvent (1.5 mL), 455–460 nm 10 W blue LEDs with fan, rt, 24 h, yield determined by <sup>1</sup>H NMR using 2,2,2-trifluoro-*N,N*-dimethylacetamide as internal standard. <sup>b</sup>40 W LEDs are used. <sup>c</sup>**1a** (0.15 mmol), **1b** (0.1 mmol), 10 W LEDs. <sup>d</sup>Isolated yield of **1c**. <sup>e</sup>Without light.

to suppress defluoroalkylation while maintaining high reactivity (entry 14). Using 1.5 equiv of **1a** with **1b** as the limiting reagent further increased the isolated yield to 88% (entry 15). Control experiments confirmed that both the Pd catalyst and light irradiation are essential, as no product formation was observed in their absence.

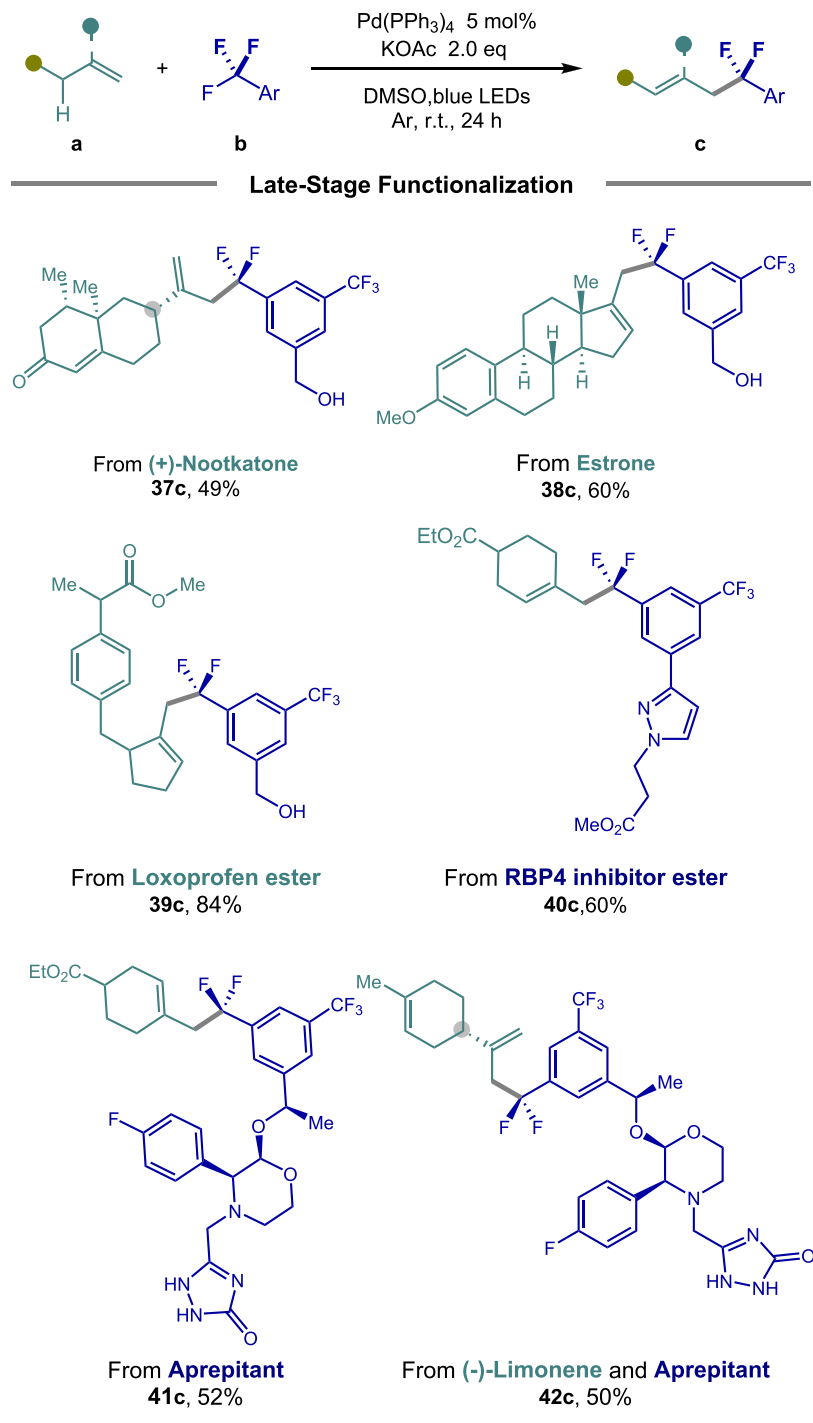
With the optimized conditions in hand, we explored the generality of this transformation (Scheme 1). Exocyclic alkenes bearing diverse functional groups, including ester (**1c**), NHBoc (**5c**), phenyl (**4c**), free hydroxyl (**6c**), and acetal (**7c**), were well-tolerated, affording the desired products (**1c**–**7c**) in yields of up to 88%. Benzoexocyclic alkenes of varying ring sizes also proved effective, yielding products (**8c**, **9c**) in 93% and 74%, respectively. Methylenecyclododecane reacted smoothly to give **10c** in 82% yield with an E/Z ratio of 1:1. Pharmaceutically relevant heterocycles, such as pyridine (**11c**), piperidine (**12c**), thiopyran (**13c**), and pyrazole (**14c**), were compatible under the optimized conditions, affording products in moderate to good yields. Acyclic 1,1-disubstituted alkenes (**15c**–**19c**) also participated, albeit with lower yields. Increasing steric hindrance led to a mixture of regioisomers (**20c**) with a ratio >10:1. 1-Phenylcyclohexene proved to be a suitable substrate, furnishing the allylic product (**21c**) in 78% yield. Notably, the more challenging linear monosubstituted alkenes (**22c**–**25c**) exhibited suitable reactivity. Next, we examined the scope of trifluoromethylarenes. Various trifluoromethylbenzenes (**26c**–**32c**) were tested, revealing that a second CF<sub>3</sub> group is essential for high reactivity, regardless of its position (meta, ortho, or para). The reaction displayed excellent functional group tolerance, accommodating tertiary amines (**26c**), free anilines (**28c**), and free phenols (**29c**), in yields up to 85%. Electron-deficient pyridines bearing a single

CF<sub>3</sub> group also performed well, yielding products (**34c**–**36c**) in 46–72%. However, the scope of trifluoromethylarenes remains limited to electron-deficient trifluoromethylarenes, because the reduction potential of the photoexcited Pd(0) catalyst is not sufficiently negative to reduce electron-neutral or electron-rich substrates via single-electron transfer. This reactivity pattern aligns with prior reports on hybrid Pd-catalyzed C–F bond cleavage, where electron-deficient arenes are necessary for efficient radical generation.<sup>11</sup> Notably, in all cases, no vinyl byproducts were detected, and only allylic products were isolated, underscoring the high regioselectivity of the β-hydride elimination step. Encouraged by these results, we explored the transformation in the late-stage functionalization of complex bioactive molecules (Scheme 2). (+)-Nootkatone, a natural sesquiterpene, underwent coupling with **1b** to afford the allylic-functionalized product **37c** in 49% yield, with complete retention of its native chirality, indicating the absence of Pd–H migration. Estrone (**38c**) and Loxoprofen (**39c**) derivatives were also compatible, yielding the corresponding allylic difluoroalkylated products in 60% and 84% yields, respectively. To further demonstrate the method's utility in drug discovery, we investigated the direct defluoroallylation of bioactive trifluoromethylated compounds. The RBP4 inhibitor (a retinoid-binding protein target) and Aprepitant (an antiemetic drug) reacted with alkene **1a**, affording defluoroallylated products (**40c**, **41c**) in moderate yields, showcasing the method's ability to modify existing drugs or prodrugs. Finally, we achieved modular cross-coupling of two complex molecules, (–)-Limonene (a terpene) and Aprepitant, yielding product **42c** in 50%. This result underscores the potential to rapidly assemble bifunctional drug-like architectures by integrating distinct pharmacophores. Notably, all transforma-

Scheme 1. Substrate Scope<sup>a</sup>

## Scheme 1. continued

<sup>b</sup>Gram scale setup. <sup>c</sup>Pd(PPh<sub>3</sub>)<sub>4</sub> (10 mol %), 456 nm (40 W). <sup>a</sup>General conditions (unless otherwise specified): a: (0.15 mmol), b: (0.1 mmol), Pd(PPh<sub>3</sub>)<sub>4</sub> (5 mol %), AcOK (0.2 mmol), DMSO (1.5 mL), 455–460 nm blue LED (10W) with fan, rt, 24 h, isolated yield.

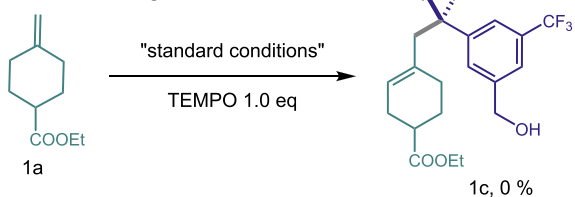
Scheme 2. Late-Stage Functionalization<sup>a</sup>

<sup>a</sup>General conditions (unless otherwise specialized): a: (0.15 mmol), b: (0.1 mmol), Pd(PPh<sub>3</sub>)<sub>4</sub> (5 mol %), AcOK (0.2 mmol), DMSO (1.5 mL), 455–460 nm blue LED with fan, rt, 24 h, isolated yield.

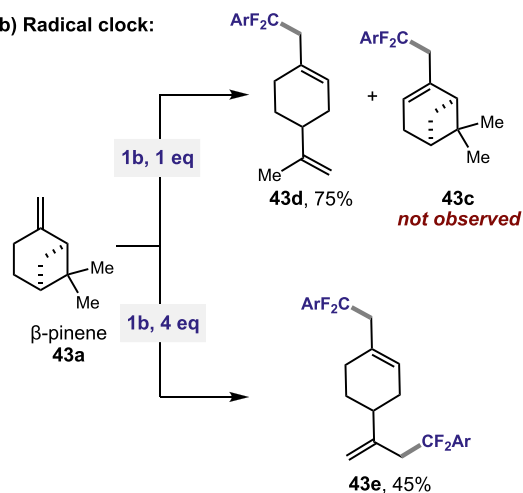
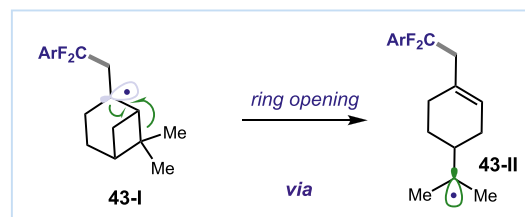
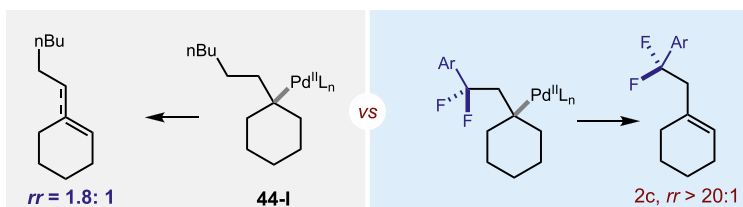
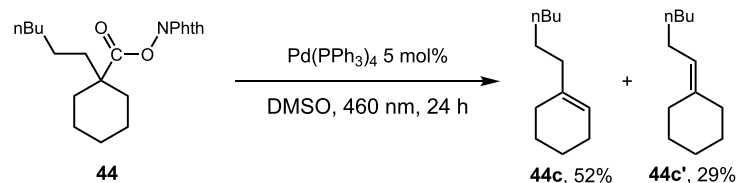
tions proceeded without racemization or decomposition of sensitive functional groups, underscoring the method's robustness and suitability for late-stage diversification in medicinal chemistry.

To elucidate the reaction mechanism, we conducted a series of control experiments and computational studies. The addition of 1.0 equiv of TEMPO completely suppressed product formation, confirming the involvement of radical

## (a) Radical Scavenger:



## (b) Radical clock:

(c) Gem-Difluoromethylene Impact on  $\beta$ -H Elimination Regioselectivity:

## (d) Gibbs free energy profile for the formation of the allylic (P1) and vinylic (P2) products

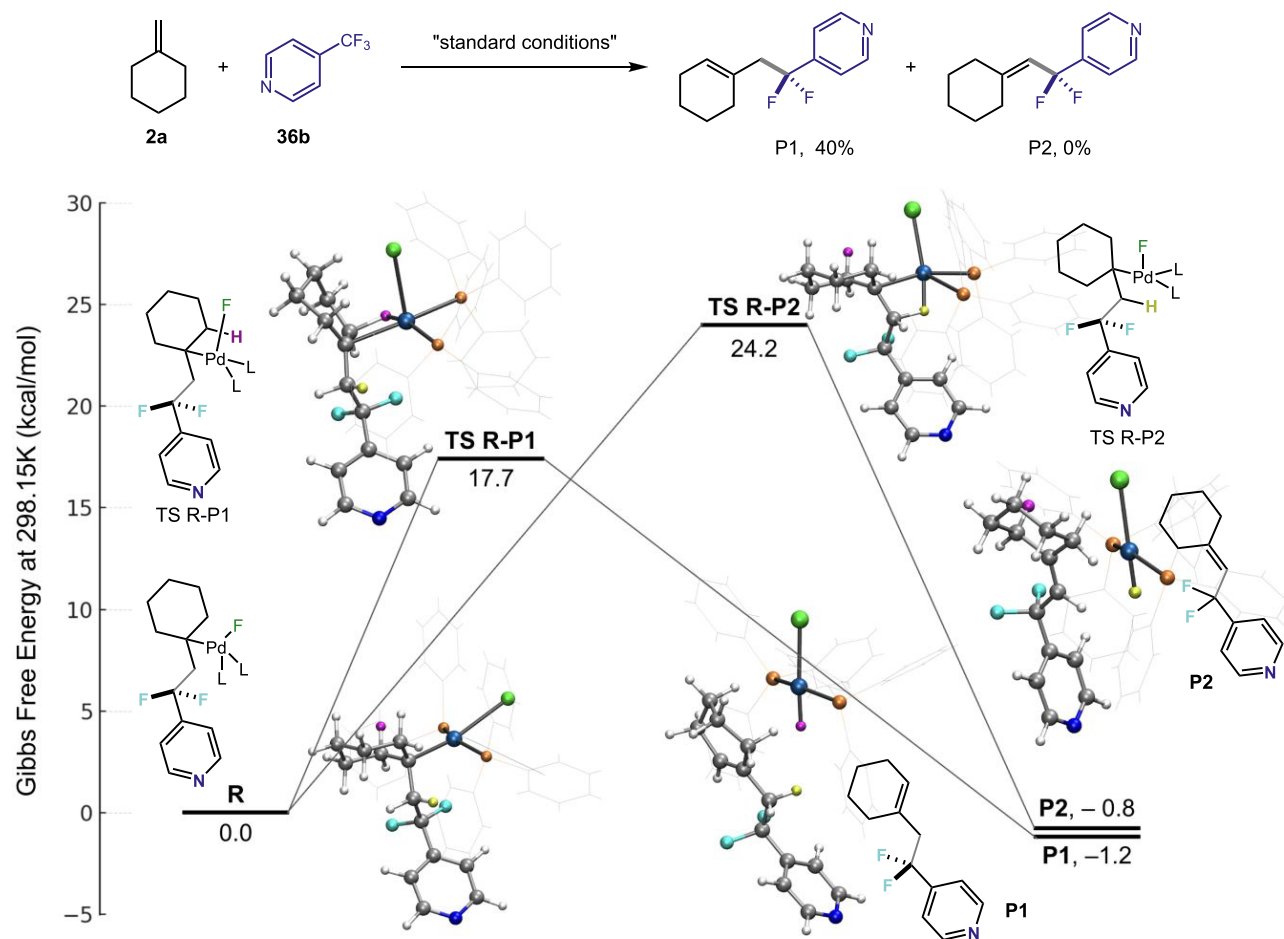


Figure 2. Mechanistic Studies.

intermediates in the catalytic cycle (Figure 2a). When  $\beta$ -pinene, a strained bicyclic alkene, was subjected to the standard conditions, the ring-opening product **43d** was obtained in 75% yield, which is consistent with radical-induced  $\beta$  C–C cleavage to relieve ring strain (Figure 2b). Increasing the Ar–CF<sub>3</sub> (**1b**) loading to 4.0 equiv facilitated further transformation of **43d**, affording **43e** in 45% yield. To investigate the role of the *gem*-difluoromethylene group, we synthesized a redox-active ester (**44**) lacking this moiety and subjected it to the reaction conditions (Figure 2c). In this case, two regioisomeric desaturation products were isolated in a 1.8:1 ratio, in contrast with the exclusive formation of the allylic product observed for substrates containing *gem*-difluoromethylene. This result highlights the critical role of the *gem*-difluoromethylene group in directing the regioselective  $\beta$ -hydride elimination.

To gain further insight into the origin of regioselectivity in the  $\beta$ -hydride elimination step, we conducted a detailed study of the potential energy surface (PES). A model substrate containing the smallest experimental substrates (methylenecyclohexane **2a** and 4-(trifluoromethyl)pyridine **36b**) was employed to make the necessary calculations tractable. Initial conformational sampling of the prereaction Pd–alkyl intermediate was carried out via CREST metadynamics simulations at the GFN2-xTB level with ALPB implicit solvation (DMSO).<sup>16</sup> Metadynamics is an enhanced sampling technique that adds history-dependent bias to a potential energy surface, thereby allowing the system to escape free energy minima and explore the underlying energy landscape. Low-energy conformers obtained from metadynamics were reoptimized at the M06-2X-D3/6-31G level of theory, and the global minimum structure was selected as the input geometry for PES exploration. All DFT optimizations were performed using NWChem at the M06-2X-D3 level of theory with the 6-31G basis set for the main group elements and the LANL2DZP effective core potential (ECP) on palladium. Potential energy surface (PES) stationary points and transition state energies were refined with single-point energies calculated at the double-hybrid DFT B2PLYP-D3/def2-TZVP level of theory. This method combination was chosen based on its demonstrated reliability in modeling both main group and transition metal systems efficiently.<sup>17–19</sup> Solvation was modeled using the COSMO continuum model with DMSO.<sup>20</sup> To probe the energetics of  $\beta$ -hydride elimination, two-dimensional constrained optimizations (0.15 Å grid spacing) were performed for each of the six accessible  $\beta$ -hydrogens in the complex – two corresponding to vinyl-type elimination and four leading to allylic products (Figures S3 and S4). The reaction coordinates were defined as the internal distances between the  $\alpha$ -carbon and palladium (C <sub>$\alpha$</sub> –Pd) and between the  $\beta$ -hydrogen and palladium (H <sub>$\beta$</sub> –Pd). From a series of constrained optimizations, the minimal energy pathways for each elimination mode were identified. The vicinity of the highest energy point on the minimal energy pathways were further refined using a higher resolution (~0.04 Å grid spacing). These points are considered as approximate to the transition states, which were subsequently reoptimized using saddle point calculations. Each transition state was confirmed by the presence of a single, relevantly large (>50 cm<sup>-1</sup>) imaginary frequency corresponding to the  $\beta$ -hydride elimination mode and was further validated by following the associated vibrational eigenvector to confirm connectivity between reactant and product through nudged minimum

energy path (MEP) descent. Figure 2d presents the reaction pathways for  $\beta$ -hydrogen elimination. The presence of the *gem*-difluoromethylene (CF<sub>2</sub>) group on the alkyl chain likely contributes to the observed regioselectivity. Electronically, CF<sub>2</sub> is inductively withdrawing and elimination to form the vinylic product would place this electron-withdrawing group closer to the developing double bond, potentially destabilizing the transition state by decreasing the favorable hyperconjugative effects.<sup>21</sup> This conclusion is supported by analysis of the relevant C–C bond during elimination: in the allylic-pathway transition state, the C–C distance is 1.42 Å, compared to 1.44 Å in the vinylic-pathway transition state, consistent with greater double bond character in the allylic case. Sterically, the CF<sub>2</sub> group and pyridine substituent introduce unfavorable interactions in the vinylic transition state geometry that are avoided in the allylic case. The crowding of the two PPh<sub>3</sub> ligands in the vinylic pathway results in an average Pd–P distance of 2.95 Å, indicating a weaker metal–ligand interaction. In contrast, the sterically less-hindered allylic transition state exhibits a shorter average Pd–P distance of 2.536 Å. This supports the conclusion that the allylic pathway is geometrically favored, with less steric strain and more effective coordination at the metal center. The transition state associated with the vinylic pathway is calculated to be 6.5 kcal/mol higher in free energy than that of the allylic pathway, while both products are modestly exergonic relative to the reactants. Given this substantial activation energy difference, the reaction is expected to proceed under kinetic control with strong selectivity for the allylic product, consistent with experimental observations.

## CONCLUSIONS

In summary, we have developed a redox-neutral, palladium-catalyzed allylic C–H difluoroalkylation of unactivated alkenes, enabled by visible-light-driven selective defluorination of trifluoromethylarenes. This method achieves mild and selective C–F bond cleavage, followed by regioselective  $\beta$ -hydride elimination from transient alkyl–Pd(II) intermediates to furnish allylic difluoroalkylated products. The *gem*-difluoromethylene group serves as a built-in regiocontrol element, distinguishing this approach from previous strategies and expanding the Mizoroki-Heck-type reactivity to include traditionally inert electrophiles. Mechanistic investigations – including radical trapping, substrate probes, and DFT-based potential energy surface analysis, support a pathway involving photoinduced Pd(0) oxidation, radical addition to alkenes, and stereoelectronically guided  $\beta$ -hydride elimination. The transformation shows broad substrate generality, including heterocycles and drug-like molecules, and enables late-stage functionalization of complex scaffolds. This work highlights how hybrid palladium catalysis can unlock new allylic C–H difluoroalkylation manifolds, setting the stage for future development of regioselective, radical-mediated C–H functionalizations.

## ASSOCIATED CONTENT

### Supporting Information

The Supporting Information is available free of charge at <https://pubs.acs.org/doi/10.1021/acscatal.5c03948>.

Full experimental procedures, spectroscopic data, and detailed X-ray crystallographic data. (PDF)

## AUTHOR INFORMATION

## Corresponding Author

Zuxiao Zhang – Department of Chemistry, University of Hawai'i at Mānoa, Honolulu, Hawai'i 96822, United States; [orcid.org/0000-0003-2365-6312](https://orcid.org/0000-0003-2365-6312);  
Email: zzhang9@hawaii.edu

## Authors

Tiancen Bian – Department of Chemistry, University of Hawai'i at Mānoa, Honolulu, Hawai'i 96822, United States

Nils W. Melbourne – Department of Chemistry, University of Hawai'i at Mānoa, Honolulu, Hawai'i 96822, United States; [orcid.org/0000-0003-0495-6790](https://orcid.org/0000-0003-0495-6790)

Yi Liu – Department of Chemistry, University of Hawai'i at Mānoa, Honolulu, Hawai'i 96822, United States

Guilhem Colomer – Department of Chemistry, University of Hawai'i at Mānoa, Honolulu, Hawai'i 96822, United States; ENS Paris-Saclay, Université Paris-Saclay, 91190 Gif-sur-Yvette, France

Rui Sun – Department of Chemistry, University of Hawai'i at Mānoa, Honolulu, Hawai'i 96822, United States; [orcid.org/0000-0003-0638-1353](https://orcid.org/0000-0003-0638-1353)

Marcus A. Tius – Department of Chemistry, University of Hawai'i at Mānoa, Honolulu, Hawai'i 96822, United States; [orcid.org/0000-0002-7092-8993](https://orcid.org/0000-0002-7092-8993)

Complete contact information is available at:  
<https://pubs.acs.org/10.1021/acscatal.5c03948>

## Author Contributions

The manuscript was written through contributions of all authors. All authors have given approval to the final version of the manuscript.

## Notes

The authors declare no competing financial interest.

## ACKNOWLEDGMENTS

We thank the Start-up Research Grant from the Department of Chemistry, University of Hawaii at Manoa for financial support. We also thank the ARPE program of ENS Paris-Saclay for supporting the internship of G.C.

## REFERENCES

- (1) For selected reviews and seminal works on allylic C–H functionalization, see: (a) Wencel-Delord, J.; Dröge, T.; Liu, F.; Glorius, F. Towards Mild Metal-Catalyzed C–H Bond Activation. *Chem. Soc. Rev.* **2011**, *40* (9), 4740–4761. (b) Dalton, T.; Faber, T.; Glorius, F. C–H Activation: Toward Sustainability and Applications. *ACS Cent. Sci.* **2021**, *7* (2), 245–261. (c) Chen, M. S.; White, M. C. Combined Effects on Selectivity in Fe-Catalyzed Methylene Oxidation. *Science* **2010**, *327* (5965), 566–571. (d) Horn, E. J.; Rosen, B. R.; Chen, Y.; Tang, J.; Chen, K.; Eastgate, M. D.; Baran, P. S. Scalable and Sustainable Electrochemical Allylic C–H Oxidation. *Nature* **2016**, *533* (7601), 77–81. (e) Zhang, F. L.; Hong, K.; Li, T. J.; Park, H.; Yu, J. Q. Organic Chemistry: Functionalization of C(sp<sup>3</sup>)-H Bonds Using a Transient Directing Group. *Science* **2016**, *351* (6270), 252–256. (f) Davies, H. M. L.; Morton, D. Guiding Principles for Site Selective and Stereoselective Intermolecular C–H Functionalization by Donor/Acceptor Rhodium Carbenes. *Chem. Soc. Rev.* **2011**, *40* (4), 1857–1869. (g) Li, J.; Zhang, Z.; Wu, L.; Zhang, W.; Chen, P.; Lin, Z.; Liu, G. Site-Specific Allylic C–H Bond Functionalization with a Copper-Bound N-Centred Radical. *Nature* **2019**, *574* (7779), 516–521.
- (2) For selected reviews on Pd-catalyzed allylic C–H functionalization, see: (a) Wang, P.-S.; Gong, L.-Z. Palladium Catalyzed

Asymmetric Allylic C–H Functionalization: Mechanism, Stereo- and Regioselectivities, and Synthetic Applications. *Acc. Chem. Res.* **2020**, *53*, 2841–2854. (b) Pàmies, O.; Margalef, J.; Cañellas, S.; James, J.; Judge, E.; Guiry, P. J.; Moberg, C.; Bäckvall, J. E.; Pfaltz, A.; Pericàs, M. A.; Diéguez, M. Recent Advances in Enantioselective Pd-Catalyzed Allylic Substitution: From Design to Applications. *Chem. Rev.* **2021**, *121*, 4373–4505 For selected examples on Pd-catalyzed oxidative C–H functionalization, see: (c) Young, A. J.; White, M. C. Catalytic Intermolecular Allylic C–H Alkylation. *J. Am. Chem. Soc.* **2008**, *130*, 14090–14091. (d) Trost, B. M.; Donckele, E. J.; Thaisrivongs, D. A.; Osipov, M.; Masters, J. T. A New Class of Non-C<sub>2</sub>-Symmetric Ligands for Oxidative and Redox Neutral Palladium-Catalyzed Asymmetric Allylic Alkylations of 1,3 Diketones. *J. Am. Chem. Soc.* **2015**, *137*, 2776–2784. (e) Lin, H. C.; Xie, P. P.; Dai, Z. Y.; Zhang, S. Q.; Wang, P. S.; Chen, Y. G.; Wang, T. C.; Hong, X.; Gong, L.-Z. Nucleophile-Dependent Z/E- and Regioselectivity in the Palladium-Catalyzed Asymmetric Allylic C–H Alkylation of 1,4-Dienes. *J. Am. Chem. Soc.* **2019**, *141*, 5824–5834. (f) Wang, H. K.; Xu, Y.; Zhang, F. Q.; Liu, Y. B.; Feng, X. M. Bimetallic Palladium/Cobalt Catalysis for Enantioselective Allylic C–H Alkylation via a Transient Chiral Nucleophile Strategy. *Angew. Chem., Int. Ed.* **2022**, *61*, No. e202115715.

(3) For selected examples involving the nucleophilic allyl transition metal intermediates, see: (a) Zhang, H.; Huang, J.; Meng, F. K. Cobalt-Catalyzed Diastereo- and Enantioselective Allyl Addition to Aldehydes and  $\alpha$ -Ketoesters through Allylic C–H Functionalization. *Cell Rep. Phys. Sci.* **2021**, *2*, No. 100406. (b) Wang, R.; Wang, Y.; Ding, R.; Staub, P. B.; Zhao, C. Z.; Liu, P.; Wang, Y.-M. Designed Iron Catalysts for Allylic C–H Functionalization of Propylene and Simple Olefins. *Angew. Chem., Int. Ed.* **2023**, *62*, No. e202216309. (c) Bao, W.; Kossen, H.; Schneider, U. Formal Allylic C(sp<sup>3</sup>)-H Bond Activation of Alkenes Triggered by a Sodium Amide. *J. Am. Chem. Soc.* **2017**, *139*, 4362–4365. (d) Zhang, X. Y.; Zheng, L.; Guan, B. T. Lithium Diisopropylamide Catalyzed Allylic C–H Bond Alkylation with Styrenes. *Org. Lett.* **2018**, *20*, 7177–7181. (e) Yamashita, Y.; Sato, I.; Fukuyama, R.; Kobayashi, S. Brønsted Base Catalyzed Imino-Ene-Type Allylation Reactions of Simple Alkenes as Uactivated Allyl Compounds. *Chem. Commun.* **2022**, *58*, 2866–2869.

(4) (a) Jeschke, P. The Unique Role of Fluorine in the Design of Active Ingredients for Modern Crop Protection. *ChemBioChem* **2004**, *5*, 570–589. (b) Hagmann, W. K. The Many Roles for Fluorine in Medicinal Chemistry. *J. Med. Chem.* **2008**, *51*, 4359–4369. (c) Müller, K.; Faeh, C.; Diederich, F. Fluorine in Pharmaceuticals: Looking beyond Intuition. *Science* **2007**, *317*, 1881–1886. (d) Kirk, K. L. Fluorine in Medicinal Chemistry: Recent Therapeutic Applications of Fluorinated Small Molecules. *J. Fluorine Chem.* **2006**, *127*, 1013–1029.

(5) For other strategies, see: (a) Schwarz, J. L.; Schäfers, F.; Tlahuext-Aca, A.; Lückemeier, L.; Glorius, F. Diastereoselective Allylation of Aldehydes by Dual Photoredox and Chromium Catalysis. *J. Am. Chem. Soc.* **2018**, *140*, 12705–12709. (b) Li, J. Y.; Zhang, Z. H.; Wu, L. Q.; Zhang, W.; Chen, P. H.; Lin, Z. Y.; Liu, G. S. Site Specific Allylic C–H Bond Functionalization with a Copper-Bound N-Centred Radical. *Nature* **2019**, *574*, 516–521. (c) Tanabe, S.; Mitsunuma, H.; Kanai, M. Catalytic Allylation of Aldehydes Using Unactivated Alkenes. *J. Am. Chem. Soc.* **2020**, *142*, 12374–12381.

(6) (a) Chu, L.; Qing, F.-L. Oxidative Trifluoromethylation and Trifluoromethylthiolation Reactions Using (Trifluoromethyl) trimethylsilane as a Nucleophilic CF<sub>3</sub> Source. *Acc. Chem. Res.* **2014**, *47*, 1513–1522. (b) Wang, J.; Luo, Z.; Wu, Y.; Tang, Y.; Yang, X.; Tsui, G. C. Copper-Catalyzed Visible-Light-Induced Allylic Difluoromethylation of Unactivated Alkenes Using Difluoroacetic Acid. *Org. Lett.* **2023**, *25* (6), 1045–1049. (c) Tagami, T.; Mitani, Y.; Kawamura, S.; Sodeoka, M. Catalytic Difluoromethylation of Alkenes with Difluoroacetic Anhydride: Reactivity of Fluorinated Diacyl Peroxides and Radicals. *Adv. Synth. Catal.* **2023**, *365* (21), 3637–3647.

(7) Wang, S.; Ren, D.; Liu, Z.; Yang, D.; Wang, P.; Gao, Y.; Qi, X.; Lei, A.-W. Cobalt-catalysed allylic fluoroalkylation of terpenes. *Nat. Synth.* **2023**, *2*, 1202–1210.

(8) Zhao, C.; Dong, C.; Ma, W.; Shi, L.; Liu, D.; Zhang, X.; Cui, Z.; Wang, Z.; Fu, J. Cobalt-Catalyzed Regiodivergent Mizoroki–Heck-Type Reaction of Simple Unactivated Alkenes. *ACS Catal.* **2024**, *14*, 14475–14485.

(9) Reviews on the hybrid palladium catalysis: (a) Chuentragool, P.; Kurandina, D.; Gevorgyan, V. Catalysis with Palladium Complexes Photoexcited by Visible Light. *Angew. Chem., Int. Ed.* **2019**, *58* (34), 11586–11598. (b) Parasram, M.; Gevorgyan, V. Visible Light-Induced Transition Metal-Catalyzed Transformations: Beyond Conventional Photosensitizers. *Chem. Soc. Rev.* **2017**, *46* (20), 6227–6240. (c) Zhou, W. J.; Cao, G. M.; Zhang, Z. P.; Yu, D. G. Visible Light-Induced Palladium-Catalysis in Organic Synthesis. *Chem. Lett.* **2019**, *48* (3), 181–191. (d) Kancherla, R.; Muralirajan, K.; Sagadevan, A.; Rueping, M. Visible Light-Induced Excited-State Transition-Metal Catalysis. *Trends Chem.* **2019**, *1* (5), 510–523. (e) Cheng, W. M.; Shang, R. Transition Metal-Catalyzed Organic Reactions under Visible Light: Recent Developments and Future Perspectives. *ACS Catal.* **2020**, *10* (16), 9170–9196.

(10) (a) Kurandina, D.; Parasram, M.; Gevorgyan, V. Visible Light-Induced Room-Temperature Mizoroki–Heck Reaction of Functionalized Alkyl Halides with Vinyl Arenes/Heteroarenes. *Angew. Chem., Int. Ed.* **2017**, *56*, 14212–14216. (b) Wang, G. Z.; Shang, R.; Cheng, W. M.; Fu, Y. Irradiation-Induced Mizoroki–Heck Reaction of Unactivated Alkyl Halides at Room Temperature. *J. Am. Chem. Soc.* **2017**, *139*, 18307–18312. (c) Kurandina, D.; Rivas, M.; Radzhabov, M.; Gevorgyan, V. Mizoroki–Heck Reaction of Electronically Diverse Tertiary Alkyl Halides. *Org. Lett.* **2018**, *20*, 357–360. (d) Zhao, B.; Shang, R.; Wang, G. Z.; Wang, S.; Chen, H.; Fu, Y. Palladium-Catalyzed Dual Ligand-Enabled Alkylation of Silyl Enol Ether and Enamide under Irradiation: Scope, Mechanism, and Theoretical Elucidation of Hybrid Alkyl Pd(I)-Radical Species. *ACS Catal.* **2020**, *10*, 1334–1343. (e) Lee, G. S.; Kim, D.; Hong, S. H. Pd-Catalyzed Formal Mizoroki–Mizoroki–Heck Coupling of Unactivated Alkyl Chlorides. *Nat. Commun.* **2021**, *12*, No. 991. (f) Wang, J.; Zhou, Q.; Zhou, L.; Zhang, Z. Pd-Catalyzed Difluoroalkylation of Alkenes Using Chlorodifluoroalkanes. *ACS Catal.* **2024**, *14*, 18499–18506.

(11) Luo, Y. C.; Tong, F. F.; Zhang, Y.; He, C. Y.; Zhang, X. Visible-Light-Induced Palladium-Catalyzed Selective Defluoroarylation of Trifluoromethylarenes with Arylboronic Acids. *J. Am. Chem. Soc.* **2021**, *143*, 13971–13979.

(12) (a) Liang, Y.; Bian, T.; Yadav, K.; Zhou, Q.; Zhou, L.; Sun, R.; Zhang, Z. Selective 1,4-Syn-Addition to Cyclic 1,3-Dienes via Hybrid Palladium Catalysis. *ACS Cent. Sci.* **2024**, *10*, 1191–1200. (b) Zhang, F.; Zhang, G.; Zhou, Q.; Bian, T.; Zhou, L.; Zhang, Z. Hybrid Palladium-Catalyzed Intramolecular Carboamination of Conjugated Dienes: Synthesis of Functionalized Pyrrolidines via Selective Trifluoromethylarene Defluorination. *J. Org. Chem.* **2024**, *89*, 7790–7794. (c) Li, Z.; Bao, L.; Wei, K.; Zhan, B.; Lu, P.; Zhang, X. Defluorinative Multicomponent Cascade Reaction of Trifluoromethylarenes via Photoexcited Palladium Catalysis. *JACS Au* **2024**, *4*, 4223–4233.

(13) Yao, W.; Mauro, J. N.; Fu, Y.; Chen, H.; Liu, P.; Ngai, M.-Y. Excited-State Palladium-Catalyzed Radical Allylic Alkylation: Rapid Access to C2-Allyl Carbohydrates. *ACS Catal.* **2025**, *15*, 5480–5489.

(14) (a) Parasram, M.; Iaroshenko, V. O.; Gevorgyan, V. Endo-Selective Pd-Catalyzed Silyl Methyl Heck Reaction. *J. Am. Chem. Soc.* **2014**, *136*, 17926–17929. (b) Fall, Y.; Berthiol, F.; Doucet, H.; Santelli, M. Palladium-Tetraphosphine Catalysed Heck Reaction with Simple Alkenes: Influence of Reaction Conditions on the Migration of the Double Bond. *Synthesis* **2007**, *2007*, 1683–1696. (c) Nishikata, T.; Ishikawa, S. Challenges in the Substitution of Terminal C–C Double Bonds with Tertiary Alkyl Groups. *Synlett* **2015**, *26*, 716–724.

(15) An illustrative example involves the use of an in situ-installed cyano group as a directing element to control the regioselectivity of  $\beta$ -hydride elimination from an alkyl–Cu(III) intermediate: Wu, X.; Riedel, J.; Dong, V. M. Transforming Olefins into  $\gamma,\delta$ -Unsaturated

Nitriles through Copper Catalysis. *Angew. Chem., Int. Ed.* **2017**, *56*, 11589–11593.

(16) Pracht, P.; Grimme, S.; Bannwarth, C.; Bohle, F.; Ehlert, S.; Feldmann, G.; Gorges, J.; Müller, M.; Neudecker, T.; Plett, C.; Spicher, S.; Steinbach, P.; Wesolowski, P. A.; Zeller, F. CREST-A program for the exploration of low-energy molecular chemical space. *J. Chem. Phys.* **2024**, *160* (160), No. 114110.

(17) Aprà, E.; Bylaska, E. J.; De Jong, W. A.; Govind, N.; Kowalski, K.; Straatsma, T. P.; Valiev, M.; Van Dam, H. J. J.; Alexeev, Y.; Anchell, J. NWChem: Past, present, and future. *J. Chem. Phys.* **2020**, *152*, No. 184102.

(18) Zhao, Y.; Truhlar, D. G. The M06 suite of density functionals for main group thermochemistry, thermochemical kinetics, non-covalent interactions, excited states, and transition elements: two new functionals and systematic testing of four M06-class functionals and 12 other functionals. *Theor. Chem. Acc.* **2008**, *120*, 215–241.

(19) Montgomery, S. L.; Ge, Y. C–H activation of ethane on palladium clusters: a computational study at the dual levels of density functional theory and coupled-cluster theory. *React. Kinet. Mech. Catal.* **2023**, *136*, 2441–2463.

(20) Klamt, A. The COSMO and COSMO-RS solvation models. *WIREs Comput. Mol. Sci.* **2018**, *8*, No. e1338.

(21) Apeloig, Y.; Rappoport, Z. The importance of hyperconjugation in nucleophilic vinylic substitution. *J. Am. Chem. Soc.* **1979**, *101*, 5095–5098.



CAS INSIGHTS™

EXPLORE THE INNOVATIONS  
SHAPING TOMORROW

Discover the latest scientific research and trends with CAS Insights. Subscribe for email updates on new articles, reports, and webinars at the intersection of science and innovation.

Subscribe today

CAS  
A Division of the  
American Chemical Society